Supporting Information

for

Superoleophilic conjugated microporous polymer nano-surfactant realizing unprecedented fast recovery of volatile organic compounds

Liang Shen[a,b,c], Wei Liu[d], Yanqiu Lu[a], Chenyi Fang[a], Sui Zhang[a,*]

[a] Department of Chemical and Biomolecular Engineering, National University of Singapore, Singapore 117576, Singapore

[b] Key Laboratory of Eco-environments in Three Gorges Reservoir Region, Ministry of Education, College of Resources and Environment, Southwest University, Chongqing 400715, China,

[c] Interdisciplinary Research Center for Agriculture Green Development in Yangtze River Basin, College of Resources and Environment, Southwest University, Chongqing, 400715, China

[d] Frontiers Science Center for Mobile Information Communication and Security, Quantum Information Research Center, School of Physics, Southeast University, Nanjing211189, China

* Corresponding author. E-mail: chezhangsui@nus.edu.sg

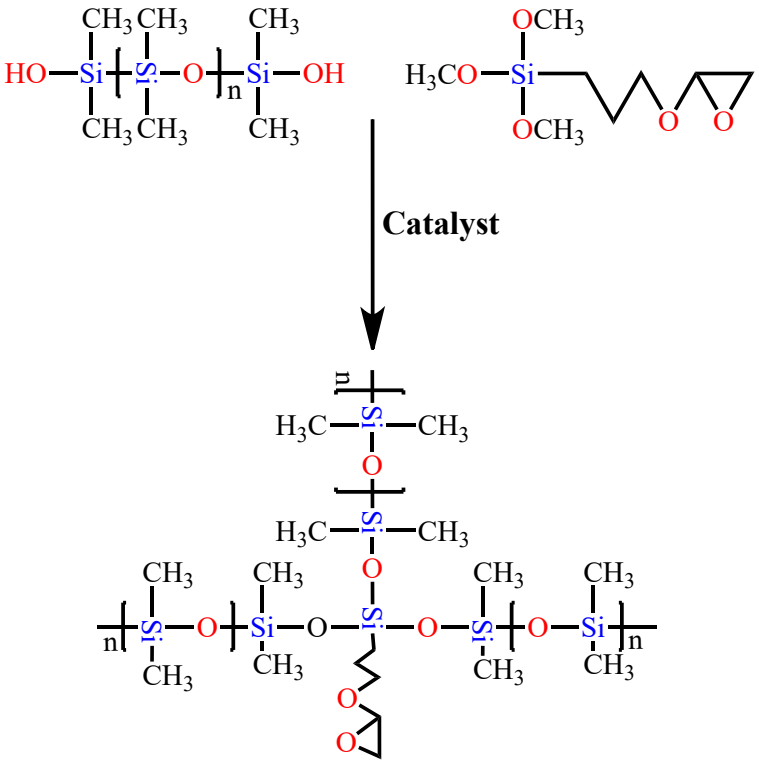

Figure S1 Chemical reaction route of PDMS crosslinking.

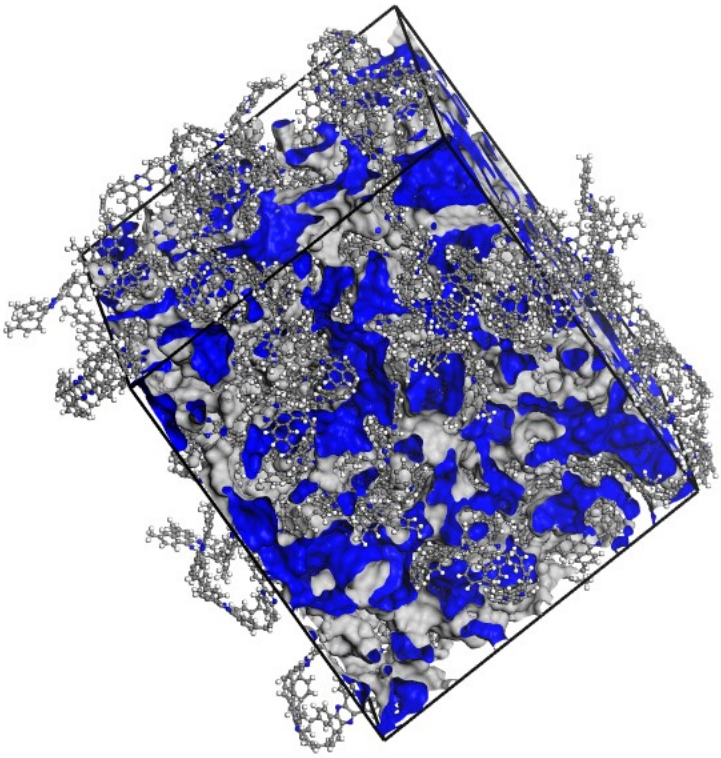

Figure S2 Constructed CMP network for pore size measurement

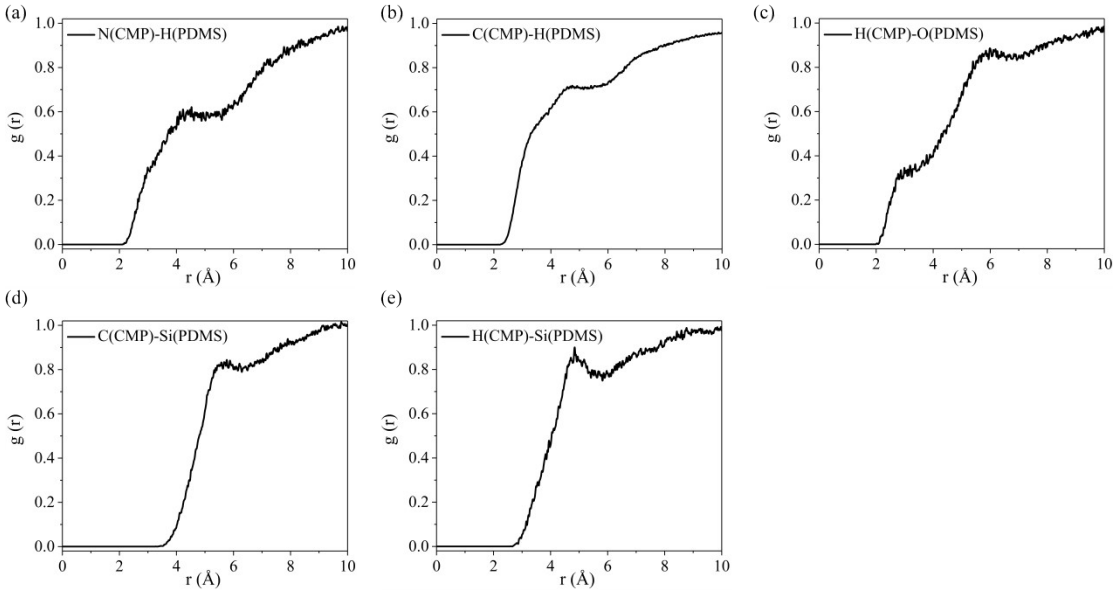

Figure S3 Radial distribution function of pairs CMP-PDMS. (a) Pairs of N(CMP)-H(PDMS), (b) pairs of C(CMP)-H(PDMS), (c) pairs of H(CMP)-O(PDMS), (d) pairs of C(CMP)-Si(PDMS), and (e) pairs of H(CMP)-Si(PDMS).

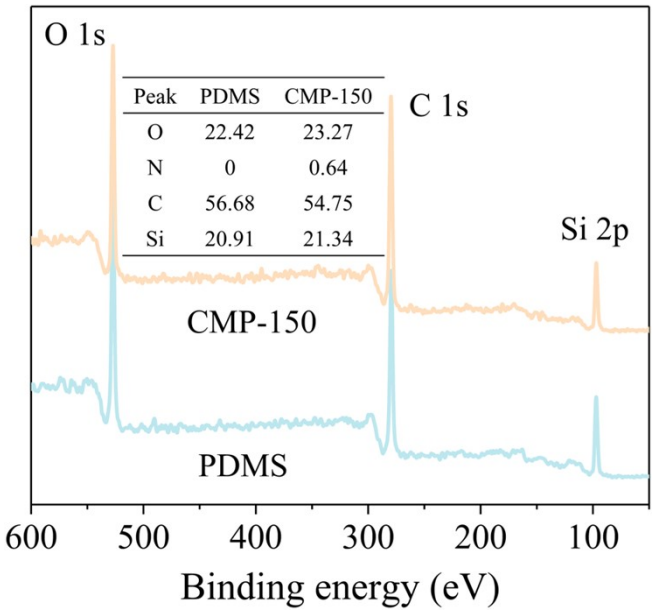

Peak	PDMS	CMP-150
O	22.42	23.27
N	0	0.64
C	56.68	54.75
Si	20.91	21.34

Figure S4 XPS spectra of PDMS and CMP-150 membranes.

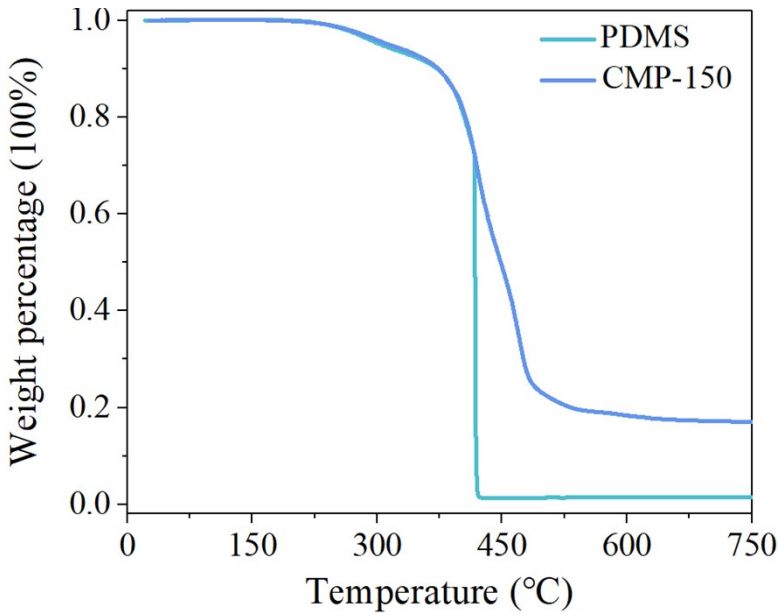

Figure S5 TGA curves of PDMS and CMP-incorporated PDMS membranes (free standing).

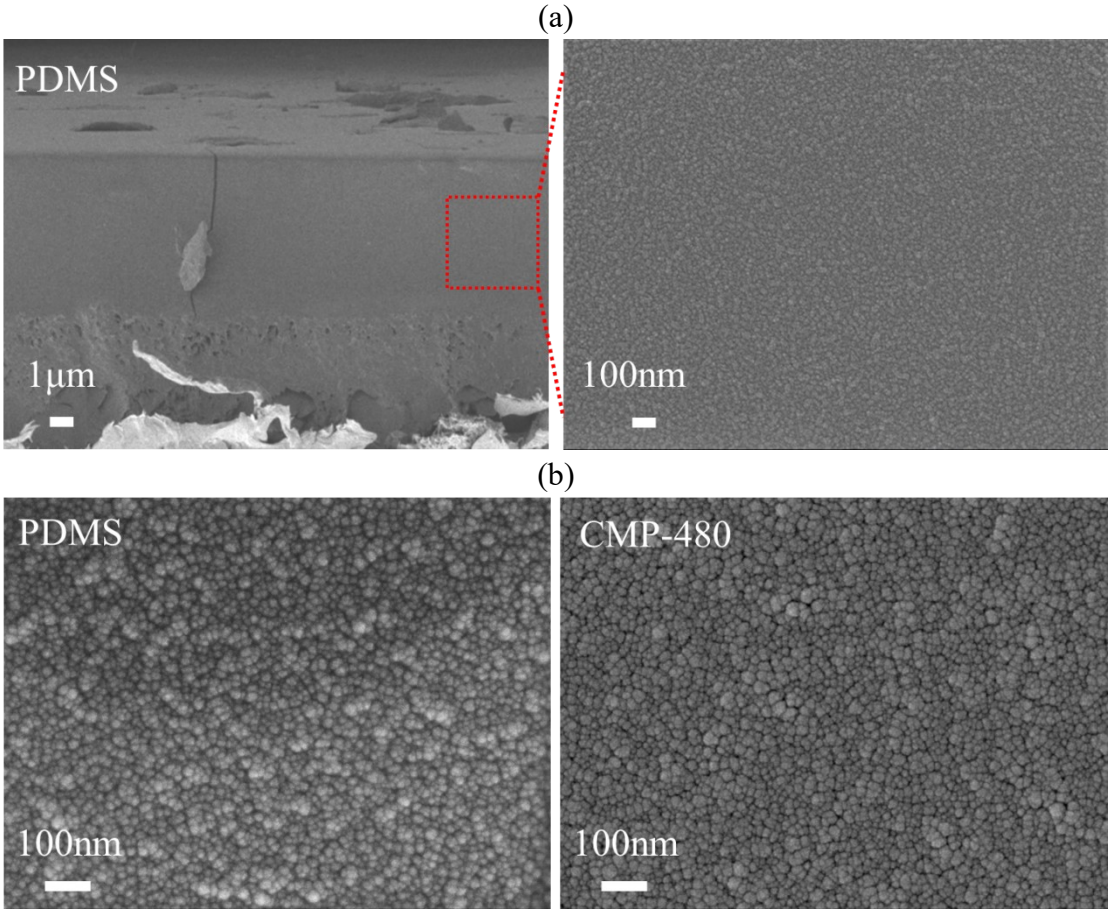

Figure S6 SEM images: (a) cross-sectional morphology of pure PDMS membrane and (b) magnified crosssectional morphology at 100 kx of PDMS and CMP-480 membranes

Rq = 1.79 nm, Ra = 1.43 nm

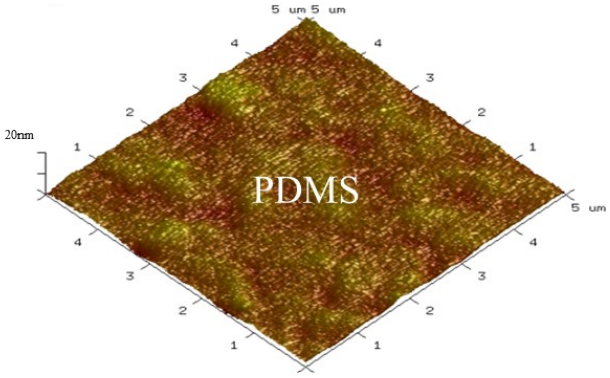

Figure S7 AFM image of PDMS membrane

Solvent uptake (SU) increment rate (IR) is define as $IR\ (\%) = \frac{SU_{n-CMP} - SU_{m-CMP}}{SU_{m-CMP}} \times 100\%$, such as $IR_{360\text{-}CMP/240\text{-}CMP}$ indicates the increment rate of 360-CMP membrane relative to that of 240-CMP membrane. It can be found in Figure S8 that when the CMP loading ≤ 240 mg L^{-1}, the increment rate of EtAc is larger than that of water due to the stronger affinity of CMP to EtAc molecules, thus the increased uptake ratios of EtAc/Water. However, when the CMP loading reaches to 360 mg L^{-1}, the free volume and pore size decreased. As a result, the smaller molecules are easier to diffuse into the denser PDMS@CMP matrix evidenced by the larger increment rate of water than that of EtAc as shown in Figure S8.

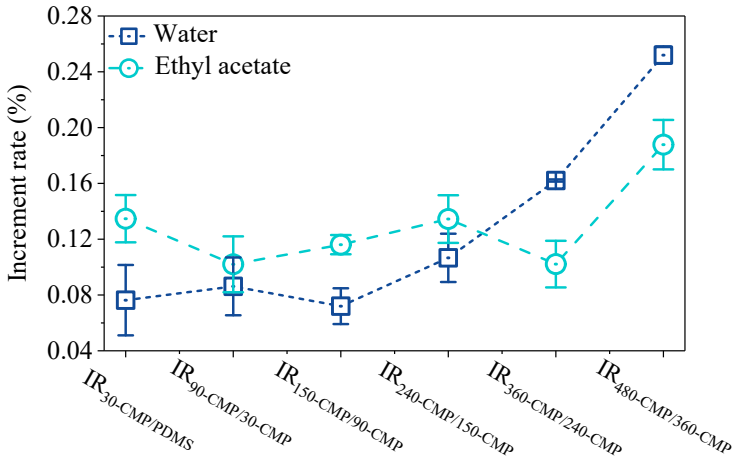

Figure S8 Solvent uptake increment rate of the CMP-incorporated and pure PDMS membranes

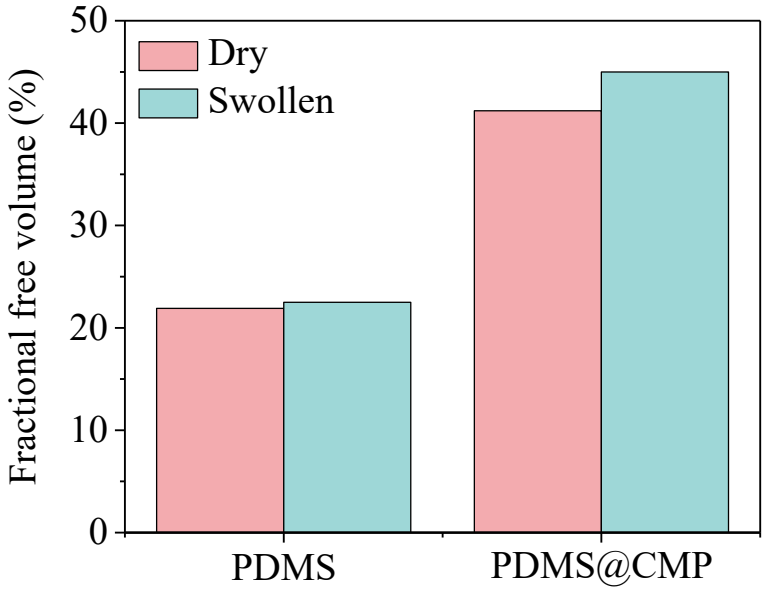

Figure S9 Fractional free volume of the pure and CMP-incorporated PDMS membranes before and after swelling by feed (5 wt% EtAc) detected by He detector.

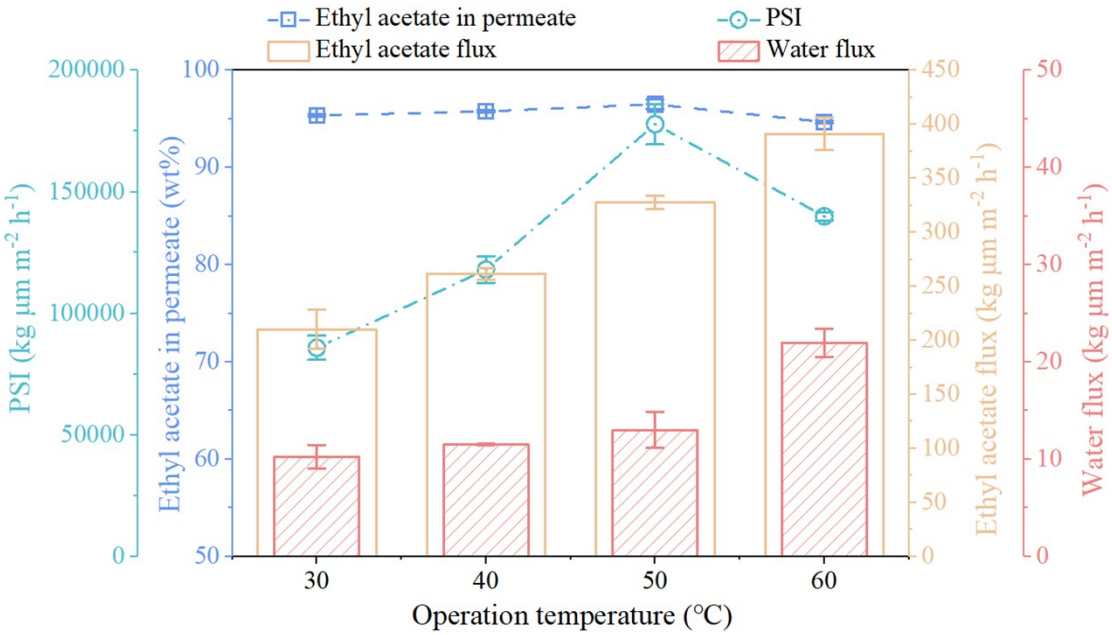

Figure S10 Pervaporation performance of CMP-150 membrane under different operation temperatures in terms of PSI, EtAc concentration in permeate, EtAc flux and water flux.

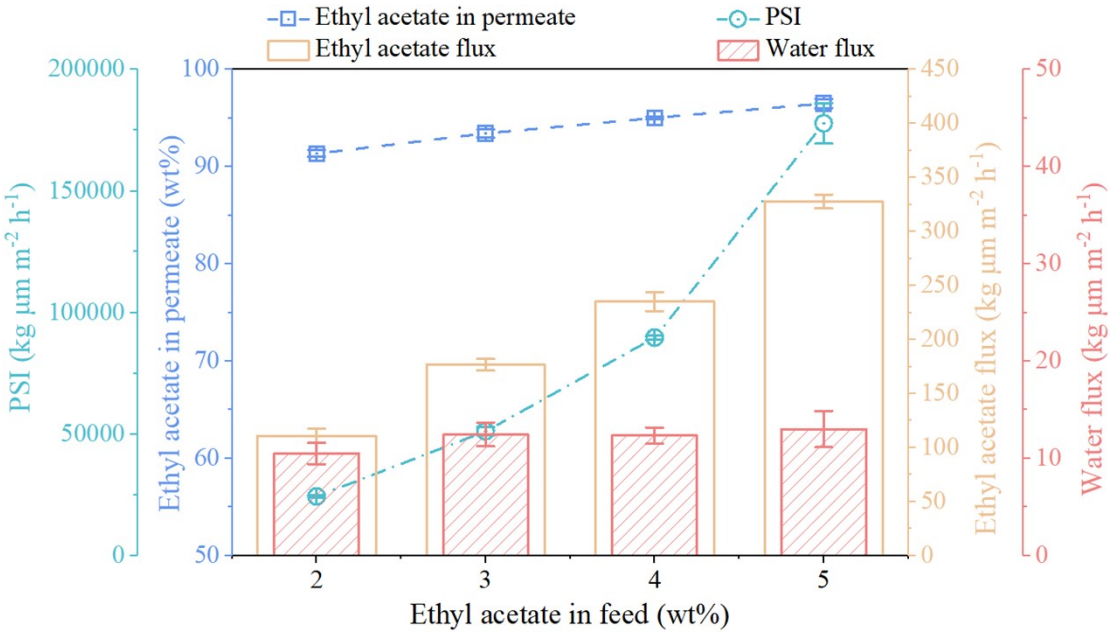

Figure S11 Pervaporation performance of CMP-150 membrane under different EtAc concentrations in terms of PSI, EtAc concentration in permeate, EtAc flux and water flux.

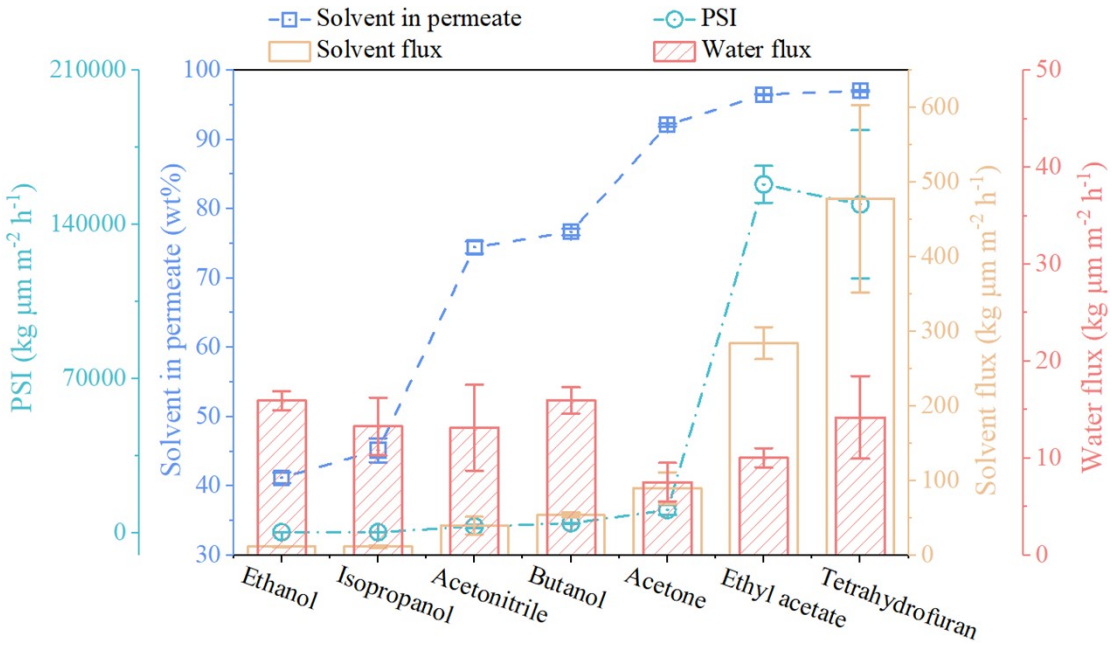

Figure S12 Pervaporation performance of CMP-150 membrane using different solvents as the feed in terms of PSI, EtAc concentration in permeate, EtAc flux and water flux.

Table S1 PALS results of the pure and CMP-incorporated PDMS membranes

Membrane	I_3(%)	FFV(%)
PDMS	25.82±0.05	11.15±0.04
CMP-150	28.44±0.05	12.41±0.05
CMP-360	24.59±0.04	10.59±0.03

According to Antoine Equation ($P = 10^{A - \frac{B}{C+T}}$), the saturated vapor pressure and partial pressure of EtAc and water in the feed can be calculated as listed in Table S2. It can be found that the increment rate of water is higher than that of EtAc, which favors the faster diffusion of water. In addition, the higher temperature results in the enlarged free volume, which also allows the faster permeation of small water molecules. These two factors both contribute to the larger increment of water flux than that of EtAc flux, and thus the decrease in separation factor at 60 ℃.

Table S2 Saturated vapor pressure and partial pressure of EtAc and water at 50-60℃

Solvent type	Saturated vapor pressure at 50℃ (kPa)	Saturated vapor pressure at 60℃ (kPa)	Partial pressure at 50℃ (kPa)	Partial pressure at 60℃ (kPa)	Partial pressure increment rate from 50℃ to 60℃ (%)
EtAc	37.986	55.827	0.405	0.595	46.91
Water	12.306	19.870	12.175	19.659	61.47

Table S3 Pervaporation performance benchmark for the recovery of EtAc from water

Membrane	Normalized total flux (Kg μm m^{-2} h^{-1})	Separation factor	Condition	Ref.
PDMS/PMHS- γ-alumina	5.3	140.0	40℃, 5wt%	15
PEBA/ZSM-5-10	40.0	102.0	30℃, 5wt%	16
ZSM-5/PEBA/PSF	37.9	108.5	50℃, 5wt%	17
HTPB-polyurethaneurea	26.5	655.0	30℃, 2.5wt%	18
P(VDF-*co*-HFP) (DMAc)	4.2	80.0	30℃, 3wt%	19
P(VDF-*co*-HFP)/PP	19	94.0	40℃, 5wt%	20
EVA38/DCE	14.4	120.0	30℃, 2.5wt%	21
Ethylene–vinyl acetate	25.0	135.0	50℃, 2.5wt%	22
PIM-1	39.5	189.0	30℃, 4.7wt%	23
PDMS (Sulzer)	18.4	76.2	40℃, 5wt%	37
PDMS/PMHS	10.4	24.0	40℃, 5wt%	37
P(VDF-*co*-HFP)/[bmim]BF_4	46.9	140.0	65℃, 5wt%	38
150-CMP	337.1	526.6	50℃, 5wt%	This work
150-CMP	273.1	431.8	40℃, 5wt%	This work
150-CMP	220.4	390.7	30℃, 5wt%	This work
240-CMP	406.2	355.5	50℃, 5wt%	This work

References

[37] M. Osorio-Galindo, A. Iborra-Clar, I. Alcaina-Miranda, A. Ribes-Greus, *Journal of Applied Polymer Science* **2001**, *81*, 546-556.

[38] D. Yongquan, W. Ming, C. Lin, L. Mingjun, *Desalination* **2012**, *295*, 53-60.